J Nanopart Res (2025) 27:171
https://doi.org/10.1007/s11051-025-06365-4

RESEARCH

Microfluidic synthesis of phosphatidylcholine liposomes for verbascoside delivery into C2C12 cells

Laura Chronopoulou · Roya Binaymotlagh · Manuela Bozzi · Marisa Colone · Anna Rita Stringaro · Francesca Sciandra · Cleofe Palocci

Received: 7 March 2025 / Accepted: 2 June 2025

Abstract The interest of lipid vesicles for applications in the pharmaceutical field is increasing, especially for preparing drug and gene delivery vectors. There are different methods for the preparation of these vesicles, however, microfluidic-based methods provide significant advantages over other synthetic protocols like extrusion and sonication. In this study, monodisperse liposomes based on L-α-phosphatidylcholine were synthesized using a versatile capillary hydrodynamic flow-focusing device to deliver verbascoside into murine C2C12 muscle cells. The size and surface charge of the obtained liposomes were studied using Dynamic Light Scattering (DLS) and zeta-potential measurements. TEM and SAXS analyses were used to investigate the shape and lamellarity of the structures. By introducing a suitable dye into the phospholipid membrane of the liposomes and using confocal fluorescence microscopic analysis, liposomes internalization in C2C12 cells was confirmed in vitro. In addition, verbascoside encapsulation in the vesicles protected it efficiently, increasing its antioxidant activity against ROS production in C2C12 cells.

Keywords Liposome vesicles · L-α-phosphatidylcholine · Verbascoside · Microfluidics · Drug delivery

L. Chronopoulou · R. Binaymotlagh · C. Palocci (✉)
Department of Chemistry, Sapienza University of Rome, Piazzale Aldo Moro 5, 00185 Rome, Italy
e-mail: cleofe.palocci@uniroma1.it
e-mail: roya.binaymotlagh@uniroma1.it

L. Chronopoulou · C. Palocci
Research Center for Applied Sciences to the Safeguard of Environment and Cultural Heritage (CIABC), Sapienza University of Rome, Piazzale Aldo Moro 5, 00185 Rome, Italy

M. Bozzi
Department of Basic Biotechnological Sciences, Intensive Clinical and Perioperative Care, Section of Biochemistry and Clinical Biochemistry, Catholic University of the Sacred Heart, Largo F. Vito 1, 00168 Rome, Italy

M. Bozzi · F. Sciandra
Institute of Chemical Sciences and Technologies "Giulio Natta" - SCITEC (CNR), Largo F. Vito, 00168 Rome, Italy

M. Colone · A. R. Stringaro
National Institute of Health, National Centre for Drug Research and Evaluation, Viale Regina Elena, 299, 00161 Rome, Italy

Introduction

Liposomes are spherical vesicles, containing an aqueous core, formed by phospholipid bilayers that are formed spontaneously when phospholipid molecules are placed in an aqueous medium. Liposomes were the first delivery systems studied, as they are able to increase the solubility of drugs and improve their pharmacokinetics [1]. Liposomes are composed of phospholipids, in particular glycerophospholipids, the constituents of eukaryotic cell membranes [2].

Published online: 16 June 2025

Different glycerophospholipids are currently used in commercial formulations such as phosphatidylcholine (PC), phosphatidylethanolamine (PE), phosphatidylserine (PS), phosphatidic acid (PA), phosphatidylinositol (PI), phosphatidylglycerol (PG) and cardiolipin (CL) [3]. PCs are an important class of glycerophospholipids present abundantly in all types of mammalian cells, subcellular organelles and some prokaryotic cells. They play a very important role in the structure of cell membranes and cell signaling. They are among the most used phospholipids in the model studies of biological membranes. There is a great variety of PCs, as the acyl chains can be subject to the action of enzymes such as phospholipases and lysophospholipid acyltransferases [4]. In particular, L-α-phosphatidylcholine (or 1,2-diacyl-sn-glycero-3-phosphocholine), is a phospholipid extracted from soy or egg yolk widely used in the production of liposomes due to its biocompatibility, biodegradability and affinity towards natural cell membranes with which it must interact for the delivery of drugs or bioactive molecules [5]. Biological applications of liposomes include their use as vectors in gene and drug delivery [6–10], as materials for carrying contrast agents in enhanced medical imaging [11], and as nano-sized crystallization reactors [12, 13]. Their structural similarities to the morphology of cells and organelles make them good model candidates for studying cellular membranes and cellular compartments like the endoplasmic reticulum and the *Golgi* apparatus [14–17]. Since the mid-90's, several liposome-based drugs have been approved for clinical use for treating diseases such as cancer, fungal and viral infections [18]. More recently, liposome-based vaccine formulations have been commercialized and used worldwide against COVID-19 spreading [19].

Conventional techniques for the preparation of liposomes, such as hydration of the thin lipid layer, solvent injection and the emulsion method, rely on the spontaneous self-assembly of particles and yield multilamellar vesicles with a heterogeneous in size distribution.. These techniques do not ensure reproducibility and size-control [20]. Furthermore, they are complex and time-consuming as post-synthesis steps (extrusion, sonication, and freeze-drying) are necessary to reduce the polydispersity in the size distribution and lamellarity of the vesicles. Obtaining a monodispersed population of liposomes is very important as it ensures a controlled dosage of the substances that will be encapsulated inside, and the control of the dimensions is necessary since the dimensions are the first factor influencing the circulation of the liposomes in the organism (clearance) and their cell internalization [21].

Microfluidics is a cutting-edge technology recently used in the production of nanoparticles, as well as liposomes [22]. Several characteristics allow us to overcome the limits imposed by conventional synthesis techniques. The laminar flow of fluids in microfluidic channels and the tunable mixing inside microfluidic reactors allow liposomes to be synthesized in a controlled and reproducible manner. In particular, by exploiting the phenomenon of hydrodynamic flow focusing, it is possible to obtain liposomes of controllable dimensions by acting on parameters such as flow speeds, flow rates, phospholipids concentration, temperature and geometric characteristics of the microfluidic reactors [23, 24].

In the present study, liposomes based on L-α-phosphatidylcholine were synthesized using a continuous flow capillary microfluidic reactor, which allowed us to investigate the effect of some operational parameters on the modulation of liposomes dimensions and polydispersion. In addition, the effect of the presence of cholesterol in the liposomal membrane in terms of structure, size, and stability of the liposomes was studied. The different liposome formulations were then used for the encapsulation of verbascoside which is a water-soluble sugar ester of caffeic acid belonging to the class of glycosidic phenylpropanoids. It is a hydrophilic compound that possesses beneficial pharmacological properties such as antioxidant, anti-inflammatory, antineoplastic, antimicrobial and neuroprotective properties [25–27]. Murine C2C12 muscle cells were treated with Verbascoside-loaded liposomes and…

Materials and methods

Materials

L-α-phosphatidylcholine (PC, from egg yolk, type XVI-E, 99%), 1,1'-dioctadecyl-3,3,3',3'tetramethy lindocarbocyanine perchlorate (Dil, 97%), Cholesterol (≥ 99%), verbascoside (VC, 99%) and all other chemicals were purchased from Sigma-Aldrich (Saint Louis, MO, USA) and used as received. Solvents

used for microfluidic syntheses were of HPLC grade and used as received from Sigma-Aldrich.

Fabrication of the microfluidic device

The microfluidic reactor used in this study consisted of three inlets, with the middle inlet designated for the organic phase, while water was injected into the two side inlets (Fig. 1). A stable hydrodynamically focused flow was achieved using a single mixing outlet channel with a fixed length of 300 mm and internal diameters of 254 µm. Precision syringe pumps (SFC300) were employed to control the flow rates of the aqueous and organic phases, using dedicated SFC software (Maxima 820, Fisons Instruments). By pumping the organic phase through the middle channel and water through the side channels, the desired flow ratio (R) was obtained, where R = organic flow rate/water flow rate.

Liposomes preparation

"Empty and VC-loaded PC liposomes were prepared using a flow-focusing microfluidic device assembled in our lab. Briefly, the reactor consists of three inlets, with the middle one designated for the organic phase, which is focused by the two side inlets, where water is typically injected. For the synthesis of empty liposomes, a stock solution of PC at a concentration of 0.76 mg/mL was prepared in ethanol, diluted to a final concentration ranging between 0.5 and 20 mM, and then injected into the central stream of the microfluidic device. Water was chosen as the continuous phase and injected into the adjacent streams. The flow rate of the continuous phase was kept constant at 2.000 µL/min, while the flow rate of the dispersed phase was varied within the 60–400 µL/min range.

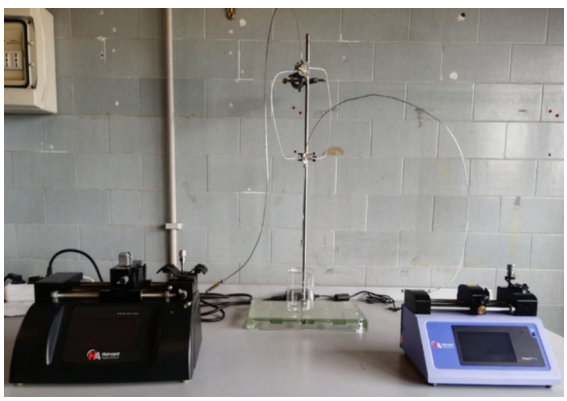

Fig. 1 Microfluidic reactor with a continuous flow system incorporating a"flow-focusing"arrangement

For the preparation of VC-loaded PC liposomes, VC was dissolved in the organic phase at a molar ratio of 2:1 (VC:PC). The flow rate ratio (FRR = flow rate of the continuous phase/flow rate of the dispersed phase) was maintained at 20 (continuous phase flow rate: 2.000 µL/min; dispersed phase flow rate: 100 µL/min). When cholesterol (Col) was used, it was dissolved in the organic phase containing PC at a w/w ratio of 1:2 (PC/Col), both for empty and VC-loaded liposomes. All experiments were performed at least in triplicate, and no precipitation was observed in the micro-channels during the experiments. The prepared liposomes were centrifuged for 40 min at 10,000 rpm, after which the pellet was redispersed in water and stored at 4 °C for further characterization.

Dynamic light scattering (DLS) and zeta potential measurement

Particle size distribution, polydispersity index (PDI), and zeta potential were measured using a Zetasizer Nano ZS (Malvern Instruments, UK), operating at $\lambda = 633$ nm with a He–Ne laser, a fixed dispersion angle of 173°, and a constant temperature of 25 °C. The experiment repeated three times.

SAXS experiments

SAXS measurements were performed at the BM29 beamline of ESRF synchrotron (Grenoble, France) with an X-ray wavelength of $\lambda = 0.992$ Å and a sample-to-detector distance of 281 cm, allowing data collection in the scattering vector range $0.07 < q < 5$ nm^{-1}. Samples were measured at 20 °C using an automatic sample changer mode of acquisition, alternating sample and blank measurements [28]. Ten subsequent 1 s exposures were collected on a Pilatus2M detector (Dectris) while flowing 70 µl of sample in the 1 mm quartz capillary, and the 2D images were masked, azimuthally averaged and converted to absolute unit scale (using water as a standard) by the automatic pipeline. Subsequent frames were checked for overlap, averaged and subtracted for the background contribution measured for the solvent.

The subtracted scattering profiles on absolute scale were compared to model intensities calculated using SasView [29] (random lamellar head/tail/tail/head sheet with Caille structure factor) and SASFit [30] (bilayered spherical vesicle model, with lognormal radius polydispersity and modified Caille multilamellar structure factor).

TEM measurements

A drop of liposome suspension was deposited onto a carbon-coated copper grid and dried at room temperature. The samples were then stained with 2% phosphotungstic acid, and excess liquid was removed using filter paper. After drying at room temperature, the samples were examined with a Philips EM 208S (FEI) TEM, which uses a W source and has a magnification power of up to 200 K. The microscope is equipped with a MegaView III camera (Olympus Soft Imaging Solutions) for image acquisition and a LEICA UC6 ultramicrotome for sectioning epoxy and acrylic resin samples.

Fourier transform infrared spectroscopy– attenuated total reflectance studies (FTIR-ATR)

FTIR-ATR data were collected with a Bruker Vertex 70 instrument (Bruker Optics, Ettlingen, Germany) using KRS-5 cells in the $4000 - 400\ cm^{-1}$ range or ATR mode on a diamond crystal in the $4000 - 600\ cm^{-1}$ spectral region.

Determination of VC encapsulation efficiency (EE)

The analytical determination of the quantity of VC trapped inside the liposomes (EE) was carried out using a spectrophotometric method. The prepared formulations were subjected to ultracentrifugation for 20 min at 6000 rpm and 4 °C to separate the liposomes from the non-entrapped VC. The supernatant was withdrawn, and its absorbance at a wavelength of 325 nm was measured and compared with a calibration line. The method was linear within the concentration range between 0.1 and 2.5 ppm of VC. The experiment was repeated three times, and finally, the %EE was calculated using the following equation:

$$\%EE = \frac{\text{total amount of VC} - \text{amount of free VC}}{\text{total amount of VC}} \times 100$$

In vitro release studies

VC-loaded liposome suspensions were placed into cellulose membranes (MWCO: 14KDa). In particular, 5 mL of each suspension was used for each sample and immersed into 25 mL of ultra-pure water inside a beaker. The samples were kept under stirring at 300 rpm and 37 °C for 7 h. At regular time intervals, 3 mL of solution outside the dialysis membrane was withdrawn and replaced with the same amount of ultra-pure water. The experiment was performed in triplicate. The absorbance of each withdrawn solution was measured with a UV–Vis spectrophotometer at 332 nm and compared with a calibration curve to calculate the amount of VC released at each time point. The experiment was repeated three times, and then, the percentage of VC release was calculated by using the following equation:

$$VCrelease(\%) = \frac{\text{released VC amount}}{\text{starting VC amount}} \times 100$$

Cell culture studies

Mouse C2C12 myoblast cells were cultured in Dulbecco's Modified Eagle Medium (DMEM, high glucose, pyruvate, phenol red, Gibco, Life Technologies, Carlsbad, CA, USA), supplemented with 10% fetal bovine serum and 10 mg/mL penicillin/streptomycin (Sigma–Aldrich, St. Louis, MO, USA), and incubated at 37 °C in humidified air with 5% CO_2.

Liposome internalization experiments

C2C12 cells were seeded onto glass coverslips and treated with Lip(PC) labeled with DiI dye, diluted in serum-free DMEM. The cells were also treated with 0.16 µM free VC and sterile water as a control. After 15, 30, and 120 min, the cells were washed with PBS, fixed with 4% paraformaldehyde for 10 min at room temperature, and imaged using a confocal laser scanning system (A1 +, Nikon, Tokyo, Japan), with laser excitation at 562 nm to collect emission signals from the DiI dye. DAPI staining

was used to visualize the nuclei. Image analysis was performed using ImageJ software, version 2.9.0

Detection of reactive oxygen species

C2C12 cells were seeded onto 24-well plates at a concentration of 0.24 $\times 10^6$ cells/well and treated with Lip(PC) and Lip(PC)@VC overnight. The production of intracellular reactive oxygen species (ROS) was evaluated using a 2',7'-dichlorofluorescin diacetate (DCF-DA)–cellular ROS detection assay kit (Abcam, Cambridge, UK). Briefly, 40 µM DCF-DA was added to liposome-treated and control C2C12 myoblasts for 45 min at 37 °C. DCF-DA is initially a non-fluorescent compound, which is deacetylated by cellular esterases to a fluorescent compound, and later oxidized by ROS into 2',7'-dichlorofluorescein (DCF), a highly fluorescent compound. After washing with PBS, cells were treated with 1 mM H_2O_2, and fluorescence was quantified every 15 min for 1 h using a multi-well plate reader (Cytation 3 Cell Imaging Multi-Mode Reader, Biotek, Canada) at excitation/emission 488/535 nm. ROS production was expressed as fluorescence intensity. Each experiment, performed in duplicate, and was repeated three times.

Results and discussion

Preparation and physicochemical characterization of PC-based liposomes

PC-based liposomes were synthesized using a continuous flow capillary microfluidic reactor with a flow-focusing configuration (Fig. 2A) [25]. The aim of this study was to synthesize liposomes with hydrodynamic diameters that can be modulated upstream of the synthetic process, a capability that cannot be achieved through post-production modifications, as is the case with conventional techniques. The significance of obtaining liposomes with adjustable and reproducible dimensions lies in their application as drug delivery nanocarriers, where size plays a crucial role in in vivo applications. To prevent their expulsion by the reticuloendothelial system (RES), the liposomes must have dimensions of less than 100 $\pm$3 nm. Figure 2(B-D) shows the experimental data related to the synthesis of liposomes with PC, either alone or in combination with Col, at a constant flow rate ratio (FRR) of 20.

The presence of sterols and in particular cholesterol in the phospholipid membrane has been widely studied to investigate its influence on the dimensions

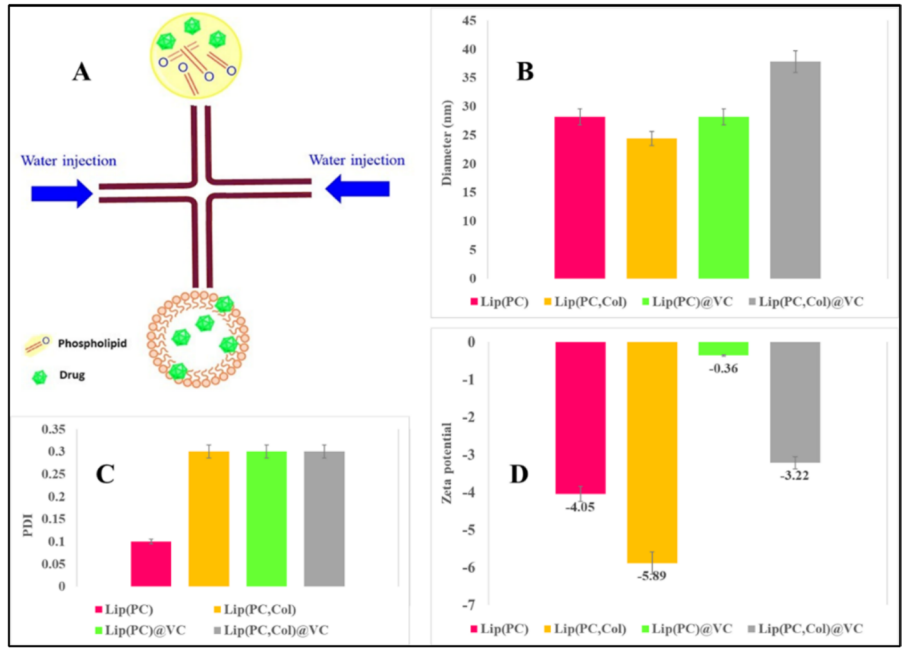

Fig. 2 **A**) Schematic representation of the preparation of PC-based liposomes using a microfluidic instrument, **B**) hydrodynamic diameter of Lip(PC) NPs in the absence and presence of VC and Col, **C**)PDI values, and D)zeta-potential of the Lip(PC) NPs in the absence and presence of VC and Col. Statistical analysis was performed using Student's t-test

and fluidity of the phospholipid membrane as well as the interactions it can establish with membrane phospholipids [31]. Liposomes were synthesized using molar ratios between PC and Col of 2:1 at FRR of 20. As shown in Fig. 1B, the presence of cholesterol leads to a decrease in the size by approximately 14%. It is known that by incorporating cholesterol into the phospholipid bilayer, it is possible to increase the order of the latter by promoting tighter packing of the chains, thanks to the steric hindrance between adjacent acyl chains formed by cholesterol. Despite this, domains rich in cholesterol and domains poor in cholesterol can be created; this may justify the increase in PDI (Fig. 2C) and therefore a lower monodispersion in the size distribution [32]. Furthermore, the hydrogen bonds between the hydroxyl groups of cholesterol and the carbonyl groups of the phospholipid molecules decrease the movement of the fatty acid chains thus decreasing the fluidity of the membrane and therefore stabilizing it. However, depending on the amount of cholesterol incorporated into the structure, it is also possible to see an increase in size accompanied by an increase in the rigidity of the phospholipid membrane [33]. Comparing the dimensions of the Lip(PC), before and after encapsulation, it is clear that the dimensions did not change significantly; on the contrary, the polydispersity index and the standard deviation on size increased, going from a highly monodisperse size distribution (PDI $\leq$ 0.1) in the case of Lip(PC), to a moderately monodisperse size distribution (0.1 $\leq$ PDI $\leq$ 0.4) in the case of Lip(PC)@VC.

On the contrary, in Lip(PC,Col) liposomes, an increase of 36% in liposome size is observed after entrapment with Verbascoside, with the size increasing from 24.4 nm to 37.8 nm in the presence of the Verbascoside molecule. This increase could be related to the incorporation of Verbascoside into the lipid bilayer, facilitated by the hydrophobic cholesterol molecule. This hypothesis could be confirmed or refuted through FTIR analysis of lipid vesicles containing cholesterol and Verbascoside, as well as by analyzing the in vitro release kinetics of Verbascoside from lipid vesicles. In the latter case, the PDI value remained unchanged, again describing a moderately monodisperse size distribution (0.1 $\leq$ PDI $\leq$ 0.4).

The zeta potential is a particularly important physicochemical parameter for describing a colloidal system. It is related to both the surface charge of the particles and their surrounding environment. Specifically, it determines the stability of the system and influences phenomena such as particle aggregation, which can alter the size, the release of encapsulated bioactive molecules, and cellular absorption. Zeta potential values between −10 mV and + 10 mV indicate unstable colloidal systems, as the electrostatic repulsion is insufficient to prevent nanoparticle aggregation [34].

From the data shown in Fig. 2D, it can be seen that, given the formation of the phospholipid bilayer, the ζ-potential of Lip(PC) is −4.05 mV, due to the presence of negatively charged phosphate groups (PO_4^{3-}) [35]. After the inclusion of cholesterol, significant changes occurred in the electrokinetic potential of the liposomes, recording a potential of −5.89 mV, probably due to the contribution of the cholesterol molecule. Finally, after the encapsulation of Verbascoside in Lip(PC), ζ-potential values closer to neutrality were obtained (−0.36 mV in the case of Lip(PC) and −3.22 in the case of Lip(PC, Col). Verbascoside could be partly included in the lipid layer with which it establishes H bonds, shielding the negative value of the lipid layer. The addition of cholesterol in the synthesis of liposomes, in which Verbascoside is trapped, allows the electrokinetic potential to be remodulated which in this case becomes more negative again.

IR spectra were recorded for the structural characterization of the liposomes, particularly to understand the behavior of Verbascoside in comparison to the phospholipid bilayer. In Fig. 3, the characteristic peaks of the structures are visible. In the characterization of PC-based liposomes (Fig. 3A), the peaks at 2922 cm^{-1} and 2849 cm^{-1} correspond to the stretching of the C-H and O–H single bonds. Peaks at 1737 cm^{-1} and 1645 cm^{-1} correspond to the stretching of the C = O bonds in the ester groups and the C = C double bonds, respectively. Finally, at 1468 cm^{-1}, the scissoring of the -CH_2 groups occurs. After the introduction of Verbascoside (Fig. 3B) into the Lip(PC), a slight shift of the peak at 1645 cm^{-1} in Lip(PC) is observed, moving to 1634 cm^{-1} after the encapsulation of Verbascoside. Considering the spectrum of Verbascoside alone (Fig. 3C), where a peak at 1634 cm^{-1} is observed, one can attribute the appearance of the peak at 1634 cm^{-1} in the spectrum of Lip(PC)@VC to the presence of Verbascoside, which is not completely encapsulated in the aqueous core but rather interacts minimally with the phospholipid bilayer.

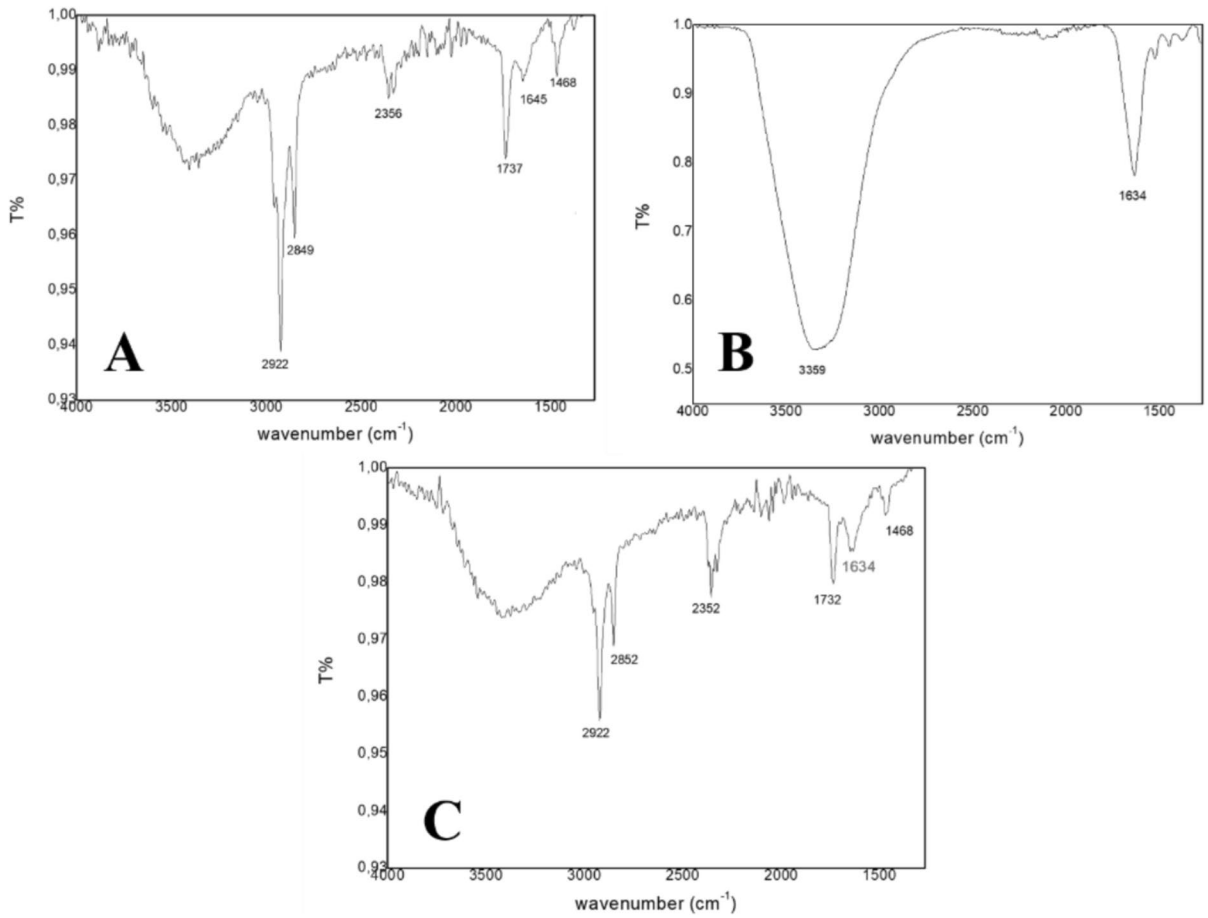

Fig. 3 ATR spectra of **A**) Lip(PC), **B**) VC, **C**) Lip(PC)@VC

Additionally, using UV–vis spectroscopy, the encapsulation efficiency (EE%) of 83.70 ±2.87% and 88.42 ±1.90% were obtained for Lip(PC) and Lip(PC,Col) NPs, respectively. These results can be interpreted as the increase in size of the Lip(PC,Col) NPs after the encapsulation of Verbascoside (Lip(PC,Col)@VC), which could also partly be distributed within the lipid bilayer, facilitated by cholesterol.

Evaluation of the lamellarity of the liposomes

The liposomes were analyzed by small-angle X-ray scattering (SAXS) and transmission electron microscopy (TEM) techniques to elucidate their internal structure, particularly their lamellarity. SAXS is a powerful technique for studying the nanostructure of liposomes, as it provides information about their shape, size, and internal organization by measuring the scattering of X-rays at small angles [36]. A model fitting was attempted for the SAXS data. As can be seen in Fig. 4A, the SAXS pattern is in agreement with a bilayer structure, which can be described in a simplified way as a 3 layer (head–tail-tail-head) electron density profile of a flat lamella, providing a form factor with a maximum around 1.4 nm^{-1}. This type of electron density profile is characteristic of lipid bilayers, where the head groups (polar regions) are positioned at the outer layers, while the hydrocarbon tails (non-polar regions) are oriented towards the inner part of the bilayer [37]. By imposing typical scattering length density (sld) values found for lipid bilayers, the head thickness is found to be 0.96 nm, and the tail thickness 1.1 nm, giving an overall bilayer thickness of (0.96 +1.1 +1.1 +0.96 =) 4.1 nm. These values align well with the bilayer thicknesses reported in various studies, which typically range from 4 to 5 nm

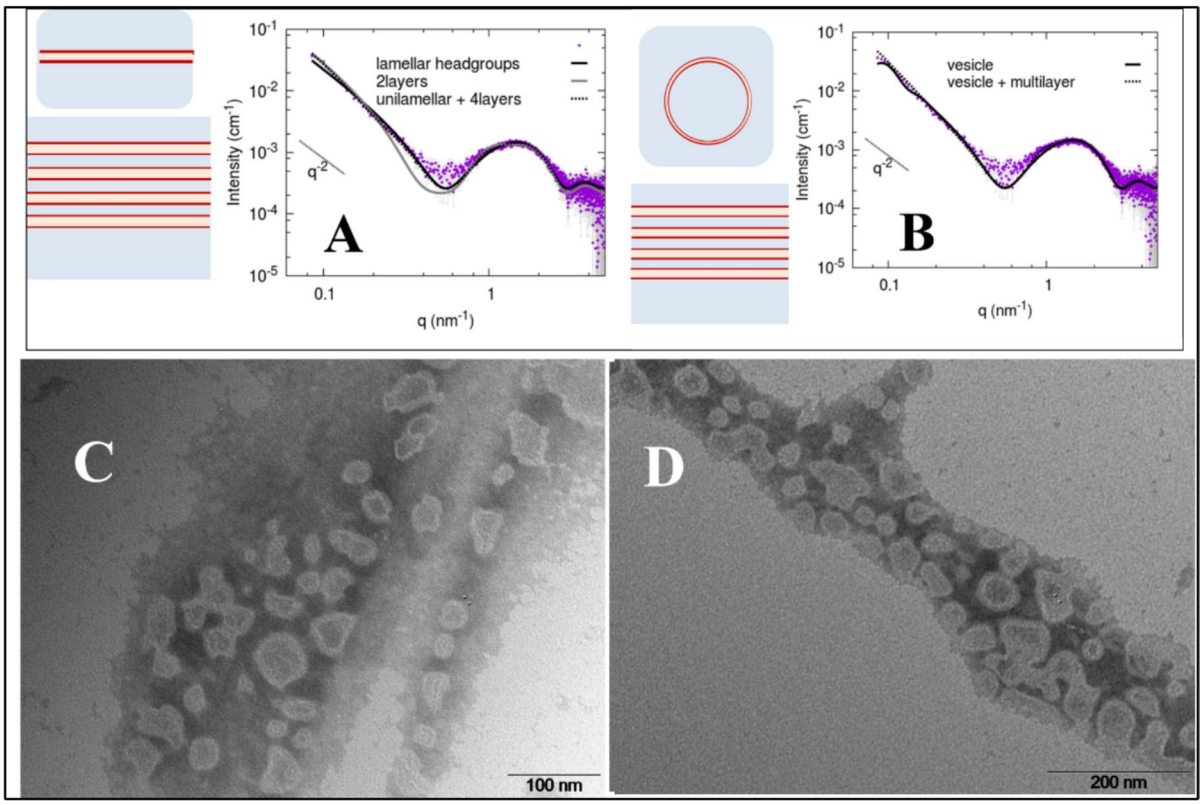

Fig. 4 SAXS profiles are based on the model fitting used for their interpretation. **A**) SAXS profile with sasview model fitting, **B**) SAXS profile with sasfit model fitting, TEM image of **C**) Lip(PC), **D**) Lip(PC, Col) NPs

depending on the lipid composition and hydration level [38]. The shoulder seen at slightly lower q (around 1 nm-1) compared to the maximum of the bilayer form factor suggests that a stacking correlation among bilayers could improve the agreement between model and data. Such a shoulder is often interpreted as indicative of bilayer stacking, where the bilayers interact with each other, resulting in periodicities in the scattering pattern [39].The improvement by considering a sum of unilamellar (73% volume fraction) and oligolamellar (27%, with N = 4 and characteristic stacking distance of 6.6 ± 0.8 nm), populations corresponds to a $\chi 2$ decreasing from 2.02 to 1.69 and is not very pronounced, suggesting that most of the sample consists of unilamellar vesicles. This observation highlights the predominance of single bilayer vesicles in the sample, a feature often observed in liposome preparations where unilamellar vesicles are the most stable form under certain conditions [40].

The spherical bilayer vesicle model implemented in the program sasfit [17] can also be used to describe the SAXS data (Fig. 4B). Sasfit is a widely used software for analyzing SAXS data, offering various models to fit data from liposomal and other complex systems [41]. In this case, the radius distribution of the spherical vesicles is an additional parameter, and we could check that small radius values around 40 nm (70–80 nm diameter) can be in agreement with the data. This is in line with typical sizes reported for liposomes in the literature, where vesicles often range from 20 to 100 nm in diameter depending on preparation method and lipid composition [42]. In addition, in this case, including a fraction of vesicles with multiple bilayers (< 4) can help describe the shoulder seen around 1 nm^{-1}. This suggests that a minor population of multilamellar vesicles may also be present in the sample, which is not unusual, as multilamellar vesicles can form during liposome preparation under

specific conditions such as excessive sonication or high lipid concentrations [43].

TEM analysis was also used as a complementary technique to confirm SAXS results. As shown in Fig. 4(C, D), Lip(PC) and Lip(PC, Col) NPs are nanometric, almost spherical, and unilamellar. The spherical morphology observed here is consistent with typical unilamellar vesicles, which are composed of a single lipid bilayer. This unilamellarity can be easily visualized using TEM imaging, where the vesicles appear as circular shapes with a clear boundary, representing the lipid bilayer [44]. Additionally, the TEM images can offer contrast between the lipid bilayer and the aqueous core of the vesicle, helping to confirm the bilayer structure [45].

No significant differences in size and morphology are evident after including cholesterol in the phospholipid membrane. This observation is in line with studies that report cholesterol's role in modulating the fluidity and packing of lipid bilayers, but not necessarily in altering the overall vesicle morphology. Cholesterol tends to stabilize the bilayer structure, increasing membrane rigidity, but it does not drastically change the vesicle size or the bilayer's appearance under TEM [46]. Furthermore, cholesterol incorporation can result in more tightly packed bilayers, which is often reflected in TEM images as vesicles with more defined and uniform bilayer edges [47]. In some cases, the presence of cholesterol can also lead to slight changes in vesicle shape, potentially affecting their size distribution, although these changes are typically subtle and can be difficult to discern with standard TEM resolution unless the cholesterol content is quite high [48].

TEM has been widely used to study liposomal formulations and is especially effective when combined with other techniques such as SAXS for a more comprehensive structural analysis. This complementary approach allows for a more robust interpretation of the liposome characteristics, particularly when determining the unilamellarity and overall size distribution of the vesicles. For instance, TEM imaging of lipid-based nanoparticles often confirms the spherical shape and unilamellar nature of the vesicles, providing direct visualization that supports SAXS-derived models of lipid bilayer thickness and internal structure [49].

In vitro release studies of verbascoside from liposomes

In vitro release studies of verbascoside from Lip(PC) and Lip(PC, Col) NPs were conducted. Figure 5 shows the kinetic trends related to the release of verbascoside over time from the liposome NPs. The percentage of verbascoside released was calculated

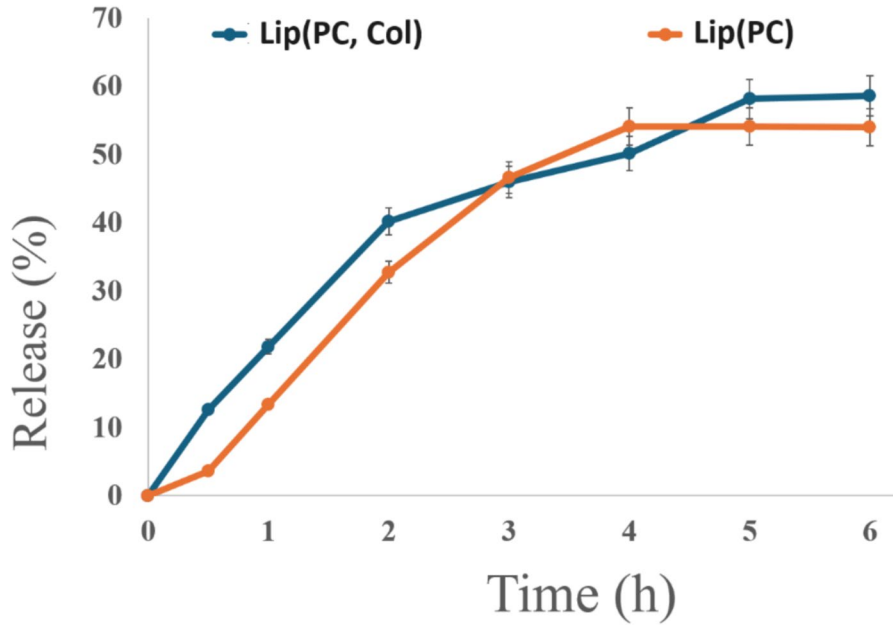

Fig. 5 In vitro release of Verbascoside from Lip(PC) and Lip(PC, Col) NPs. Statistical analysis was performed using Student's t-test

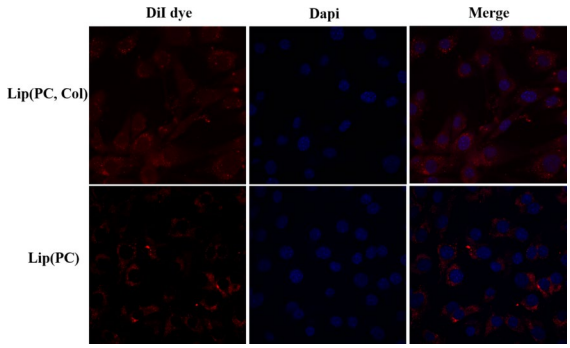

Fig. 6 Representative fluorescence images of C2C12 myoblasts after 15 min of treatment with Lip(PC, Col) and Lip(PC) labeled with DiI dye. Red fluorescence DiI dye signal shows that NPs entered inside the cytoplasm. Nuclei were stained with DAPI

by analyzing the absorbance values obtained from spectrophotometric measurements. Concentrations were determined using a calibration curve, allowing for the quantification of the released amount relative to the total. In the first 2 h of incubation, the release rate of VC from Lip(PC, Col) significantly exceeded that from Lip(PC) by 25% (Fig. 5). After 5 h, in both cases, the release trend reached a plateau, with release percentages of 54.11% for Lip(PC) NPs and 58.6% for Lip(PC, Col) NPs, which remained constant until the sixth hour.

Biological studies: Cellular uptake of Lip(PC) and Lip(PC, Col) NPs

The internalization of liposomes in murine muscle cells was studied. Figure 5 shows the fluorescence microscopy images of murine myoblasts that have internalized liposomes containing the fluorescent probe in their membranes. After 15 min of contact, Lip(PC) and Lip(PC, Col) NPs labeled with DiI dye were internalized by murine C2C12 muscle cells. They are present in the cytoplasm and nucleus (Fig. 6); however, they are not observed on the plasma membrane, suggesting that a possible endosomal uptake pathway mediates the cellular internalization of Lip(PC). Further analysis will be required to better clarify the mechanism of Lip(PC) uptake.

ROS production assay

The release of VC from liposomes in murine muscle cells was analyzed by measuring the ability of VC to counteract the production of H_2O_2-induced ROS. The DCF-DA assay was carried out on C2C12 myoblasts pre-treated with Lip(PC)@VC, Lip(PC), and free VC [24]. After the addition of DCF-DA, cells were exposed to 1 mM H_2O_2, and the fluorescence induced by ROS production was recorded every 15 min. Figure 7A shows that Lip(PC) enhances the delivery of VC to cells, as Lip(PC)@VC exhibits a higher anti-ROS activity compared to free VC.

As can be seen in Fig. 7B, VC delivered by Lip(PC) decreased the intracellular production of ROS in comparison to the untreated cells and cells treated with free VC which reveals NPs can protect VC molecules from degradation and release them gradually over time.

Conclusions

In this work, a hydrodynamic flow-focusing (HFF) device was used to synthesize liposome NPs with a specific size using L-α-phosphatidylcholine lipids to encapsulate the antioxidant glycosidic phenylpropanoid, verbascoside (VC) (Lip(PC)@VC). Additionally, its effect on size, zeta potential, and PDI was studied. It was demonstrated that unilamellar NPs of approximately 30 nm were successfully synthesized and could encapsulate VC molecules with an efficiency of 83.70 ±2.87%. The Lip(PC)@VC NPs were internalized by murine C2C12 muscle cells, and their effectiveness in counteracting ROS production in C2C12 cells was investigated. It was shown that Lip(PC) NPs can protect VC molecules from degradation and exhibit significant antioxidant activity. Lip (PC, Col) demonstrated higher encapsulation efficiency (EE) and faster in vitro drug release than Lip(PC); however, in terms of cellular uptake and ROS reduction, Lip(PC) NPs showed better performance.

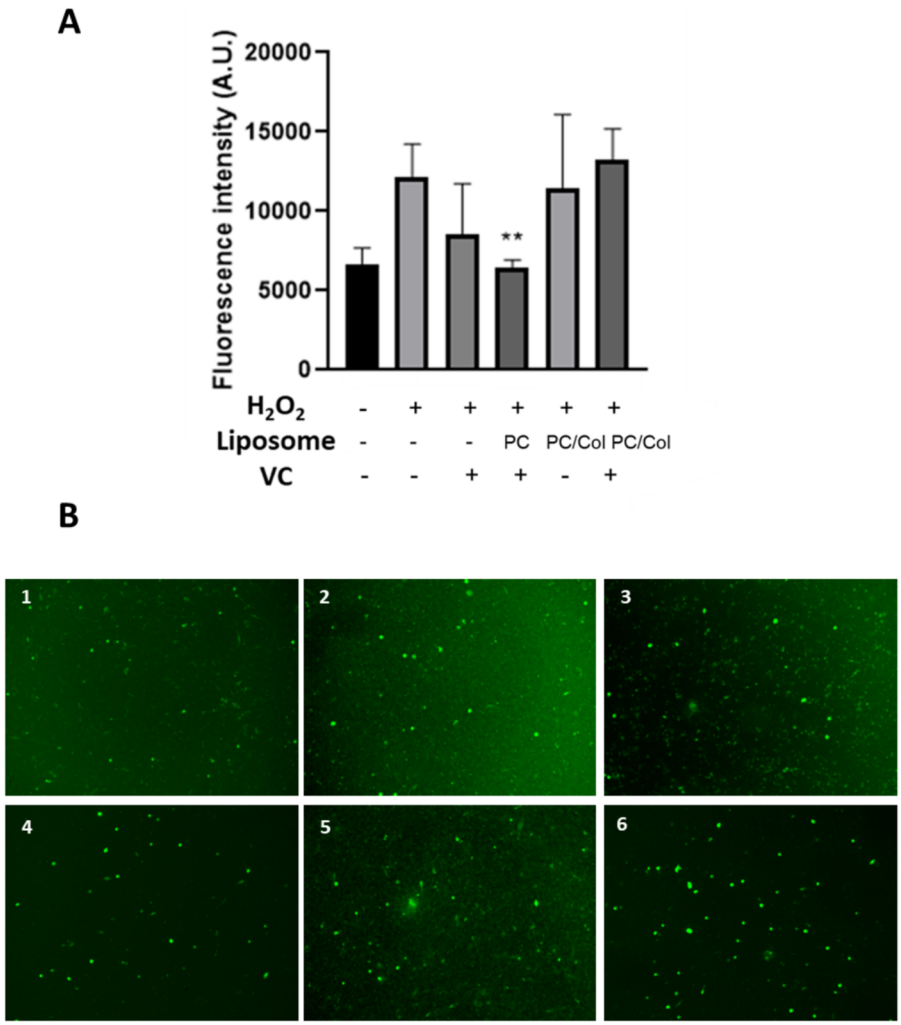

Fig. 7 **A)** ROS production assay. Oxidative stress was induced with 1 mM H_2O_2 in C2C12 myoblasts untreated and treated with free VC (0.16 mM) or VC loaded in Lip(PC) and Lip(PC, Col). Intracellular ROS induce oxidation of 2',7'-dichloro-fluorescin developing a fluorescent compound whose concentration is directly proportional to the amount of ROS. **B)** Representative fluorescence images of 1) untreated cells, 2) cells incubated with H_2O_2, cells stressed with H_2O_2 and treated with 3) free VC, 4) Lip(PC)@VC, 5) Lip(PC, Col) and 6) Lip(PC, Col)@VC. Fluorescence intensity is expressed in arbitrary units (A.U.). Statistical analysis was performed using Student's t-test (** $p \leq 0.01$, H_2O_2/Lip(PC)@VC-treated cells vs. H_2O_2-treated cells)

Author contributions The manuscript was written with contributions from all authors. All authors have approved the final version of the manuscript."L.C.: provided paper Conceptualization, Methodology, Investigation and she Writed-Original Draft. R. B. wrote the paper in terms of conceptualization and Methods, she investigated, and wrote the Original Draft. M. B. took care the section Methodology, Formal Analysis and Data Curation. F. S.: wrote the section methodology, and carried out Formal Analysis, revising Data obtained. C. P.: she took care of Conceptualization, revision of Methodology section, Writing—and final Review and Editing, supervised the final version, and Funding acquisition. M. C. and A.R. S. took care Methodology section.

Funding The authors thank for funding the Ateneo Sapienza 2024 project n. RG124190E4DF3504.

Data availability No datasets were generated or analysed during the current study.

Compliance with ethical standards

Competing interest The authors declare no competing interests.

References

1. Binaymotlagh R, HajarehHaghighi F, Chronopoulou L, Palocci C (2024) Liposome-Hydrogel composites for controlled drug delivery applications Gels 10:284
2. Tang J et al (2021) Liposome interaction with macrophages and foam cells for atherosclerosis treatment: effects of size, surface charge and lipid composition. Nanotechnology 32:505
3. Atre P, Rizvi SAA (2024) A brief overview of quality by design approach for developing pharmaceutical liposomes as nano-sized parenteral drug delivery systems. RSC Pharm 1:675–688
4. Van Der Veen JN, Kennelly JP, Wan S, Vance JE, Vance DE, Jacobs RL (2017) The critical role of phosphatidylcholine and phosphatidylethanolamine metabolism in health and disease Biochim. Biophys Acta 1859:1558
5. Marrapu B, Mallampalli LK, Kaki SS, Rachapudi BNP (2015) A novel method to synthesize 1-acyl-sn-glycero-3-phosphocholine and 1,2-diacyl- sn -glycero-3-phosphocholine. Eur J Lipid Sci Technol 117:1049
6. Nsairat H, Khater D, Sayed U, Odeh F, Bawab AA, Alshaer W (2022) Liposomes: structure, composition, types, and clinical applications. Heliyon 8:e09394
7. Yamada M, Takizawa T, Kikuchi H (2008) Development of MITO-Porter: A liposome-based carrier system for delivering macromolecules into mitochondria via membrane fusion. J Nanopart Res 10:741
8. Crosasso P, Ceruti M, Brusa P, Arpicco S, Dosio F, Cattel L (2000) Preparation, characterization and properties of sterically stabilized paclitaxel-containing liposomes. J Control Release 3:19–30
9. Mayer LD, Krishna R, Webb M, Bally M (2000) Designing liposomal anticancer drug formulations for specific therapeutic applications. J Liposome Res 10:99–115
10 Ramachandran S, Quist AP, Kumar S, Lal R (2006) Cisplatin nanoliposomes for cancer therapy: AFM and fluorescence imaging of cisplatin encapsulation, stability, cellular uptake, and toxicity. Langmuir 22:8156–62
11. Musielak M, Potoczny J, Boś-Liedke A, Kozak M (2021) The combination of liposomes and metallic nanoparticles as multifunctional nanostructures in the therapy and Medical Imaging-A review. Int J Mol Sci 22:6229
12. Pilkington CP, Gispert I, Chui SY, JohnM S, Elani Y (2024) Engineering a nanoscale liposome-in-liposome for in situ biochemical synthesis and multi-stage release. Nat Chem 16:1612
13. Korgel BA, Monbouquette HG (1999) Controlled synthesis of mixed core and layered (Zn, Cd)S and (Hg, Cd)S nanocrystals within phosphatidylcholine vesicles. Langmuir 15:1611
14. Tamura T et al (2020) Organelle membrane-specific chemical labeling and dynamic imaging in living cells. Nat Chem Biol 16:1361
15 Stano P, Kuruma Y, Souza TP, Luisi PL (2010) Biosynthesis of proteins inside liposomes. Methods Mol Biol 606:127–45
16. Görlich D, Rapoport TA (1993) Protein translocation into proteoliposomes reconstituted from purified components of the endoplasmic reticulum membrane. Cell 75:615–630
17. Pécheur EI, Martin I, Maier O, Bakowsky U, Ruysschaert JM, Hoekstra D (2002) Phospholipid species act as modulators in p97/p47-mediated fusion of Golgi membranes. Biochemistry 41:9813–23
18 Nsairat H, Khater D, Sayed U, Odeh F, Al Bawab A, Alshaer W (2022) Liposomes: structure, composition, types, and clinical applications. Heliyon 13:e09394
19 Gregoriadis G (2021) Liposomes and mRNA: Two technologies together create a COVID-19 vaccine. Med Drug Discov 12:100104
20. Aranguren A, Torres CE, Muñoz-Camargo C, Osma JF, Cruz JC (2020) Synthesis of nanoscale liposomes via low-cost microfluidic systems. Micromachines 11:1050
21. Jahn A, Reiner JE, Vreeland WN, DeVoe DL, Locascio LE, Gaitan M (2008) Preparation of nanoparticles by continuous-flow microfluidics. J Nanopart Res 10:925
22. Orekhova A, Palocci C, Chronopoulou C, De Angelis G, Badiali C, Petruccelli V, D'Angeli S, Pasqua G, Simonetti G (2022) Poly-(lactic-co-glycolic) acid nanoparticles entrapping pterostilbene for targeting aspergillus section nigri. Molecules 27:5424
23. Van Swaay D, deMello A (2013) Microfluidic methods for forming liposomes. Lab Chip 13:52
24. Yu B, Lee RJ, Lee LJ (2009) Microfluidic methods for production of liposomes. Methods Enzymol 465:129–141
25. Alipieva K, Korkina L, Orhan IE, Georgiev MI (2014) Verbascoside-A review of its occurrence, (Bio)synthesis and pharmacological significance Biotechnol. Adv 32:1065
26. Funes L, Laporta O, Cerdán-Calero M, Micol V (2010) Effects of verbascoside, a phenylpropanoid glycoside from lemon verbena, on phospholipid model membranes. Chem Phys Lipids 163:190–9
27. Sciandra F, Bozzi M, Bigotti MG (2023) From adhesion complex to signaling hub: the dual role of dystroglycan. Front Mol Biosci 10:1325284
28. Round A et al (2015) BioSAXS Sample Changer: a robotic sample changer for rapid and reliable high-throughput X-ray solution scattering experiments. Acta Crystallogr D Biol Crystallogr 71:67
29. Burlew M (2005) SAS Guide to Report Writing Examples, 2nd edn. SAS Institute
30. Breßler I, Kohlbrecher J, Thünemann AF (2015) sasfit : a tool for small-angle scattering data analysis using a library of analytical expressions. J Appl Crystallogr 48:1587
31. Briuglia ML, Rotella C, McFarlane A, Lamprou DA (2015) Influence of cholesterol on liposome stability and on in vitro drug release. Drug Deliv Transl Res 5:231
32. Kaddah S, Khreich N, Kaddah F, Charcosset C, Greige-Gerges H (2018) Cholesterol modulates the liposome membrane fluidity and permeability for a hydrophilic molecule. Food Chem Toxicol 113:40
33. Chen W, Zou M, Ma X, Lv R, Ding T, Liu D (2019) Co-encapsulation of egcg and quercetin in liposomes for optimum antioxidant activity. J Food Sci 84:111

34. Bhattacharjee S (2024) DLS and zeta potential-What they are and what they are not? J of Cont Release 235:337
35. Zhou F et al (2018) Chitosan-coated liposomes as delivery systems for improving the stability and oral bioavailability of acteoside. Food Hydrocoll 83:17
36. Pabst G et al (2006) Small-angle X-ray scattering from model membranes. Biochim Biophys Acta - Biomembr 1758:1443
37. Israelachvili JN (2011) Intermolecular and surface forces. Academic Press
38. Marsh D (2008) Physical chemistry of lipids: From fatty acids to phospholipids. Springer SBM
39. Chabre Y et al (1994) Scattering from multilamellar and unilamellar vesicles. Biochim Biophys Acta - Biomembr 1222:193
40. Kato M et al (1995) Stability of unilamellar vesicles prepared by extrusion and sonication. Biophys J 69:1856
41. Salditt T et al (2009) SASFit: A software for the analysis of small-angle scattering data from liposomal and other complex systems. J Appl Crystallogr 42:1082
42. Hwang S et al (2005) Characterization of liposomal formulations: size, polydispersity, and stability. Langmuir 21:5167
43. Sessa G et al (1974) Multilamellar vesicles in liposome preparations: formation, properties, and behavior. Biochem Biophys Res Commun 58:1194
44. Barenholz Y (2015) Liposome applications: Review of current medical research. Nanomed Nanotechnol Biol Med 11:1
45. Popova NL et al (2000) Application of transmission electron microscopy to study liposome-based drug delivery systems. Micron 31:385
46. Waring AJ et al (1993) The role of cholesterol in lipid membranes and liposomal formulations. Biophys J 65:57
47. Ipsen JH et al (1987) Phase equilibria of phospholipid bilayers: theory and experiments. Biochimica et Biophysica Acta - Biomembranes 905:162
48. Almeida PF et al (1995) Modulation of lipid bilayer properties by cholesterol: Effects on the bilayer's mechanical and structural properties. Biochim Biophys Acta (BBA) Biomembranes 1241:313
49. Brown WK et al (2006) Electron microscopy techniques for liposomal formulations. Colloids Surf B Biointerfaces 50:6